

# The Preparation of Supported NiO and Co<sub>3</sub>O<sub>4</sub> Nanoparticles by the Nitric Oxide Controlled Thermal Decomposition of Nitrates

Jelle R. A. Sietsma, Johannes D. Meeldijk, Johan P. den Breejen, Marjan Versluijs-Helder, A. Jos van Dillen, Petra E. de Jongh, and Krijn P. de Jong\*

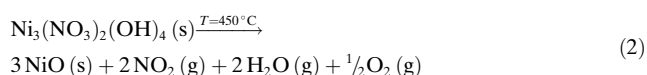
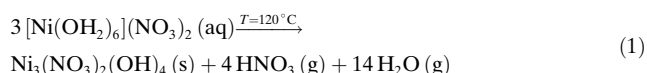
Metal (oxide) nanoparticles smaller than about 20 nm have received widespread interest recently because of their envisioned applications in electronics, optics, and magnetic storage devices.<sup>[1]</sup> They are currently used as catalysts for the production of fuels and chemicals and the reduction of environmental pollution.<sup>[2]</sup> High surface-to-volume ratios are important for these particles since catalytic processes take place at the metal (oxide) surface; therefore supports such as SiO<sub>2</sub> and Al<sub>2</sub>O<sub>3</sub> are generally used to obtain small and thermally stable particles. Furthermore, the use of inert matrices allows the design of materials for specific applications, such as drug-delivery systems.<sup>[3]</sup>

Small particles on a support material can be obtained by deposition from the vapor or liquid phase,<sup>[4]</sup> and the most widely used method is based on impregnation of a porous support with a precursor-containing solution, followed by drying. Subsequent thermal treatment in air converts the precursor into the desired metal oxide or metal if followed by high-temperature reduction. Particles with diameters of 1–3 nm can be deposited from organic precursor complexes, but their limited solubility allows only moderate loadings (≤10 wt %) by single-step impregnations;<sup>[5]</sup> therefore inorganic salts are typically used to achieve higher metal oxide loadings. Nitrates, in contrast to chlorides and sulfates, are the most commonly used salts, because they can be fully converted into the corresponding oxides. However, supported metal oxides prepared from nitrates generally display relatively large particle sizes.<sup>[5–7]</sup>

Herein we present a new method that allows the preparation of uniform and small metal oxide particles based on impregnation with aqueous metal nitrate solutions. We describe nickel on silica as an example, but also show the relevance of this method for other systems. Moreover, the significance of these nanoparticles for catalysis is illustrated by the activity of Co/SiO<sub>2</sub> in the Fischer–Tropsch synthesis of hydrocarbons.<sup>[8]</sup>

The formation of NiO from aqueous nickel nitrate solution involves two steps: deposition of Ni<sub>3</sub>(NO<sub>3</sub>)<sub>2</sub>(OH)<sub>4</sub>

during drying [Eq. (1)] and subsequent decomposition of this compound into NiO [Eq. (2)].



We studied the impact of each individual step in the preparation procedure using ordered mesoporous silica SBA-15 as a model support.<sup>[9]</sup> Dark-field scanning transmission electron microscopy (STEM) images of the samples recorded with a high angular annular dark field (HAADF) detector are shown in Figure 1.<sup>[10]</sup> After drying at 120 °C (center image),

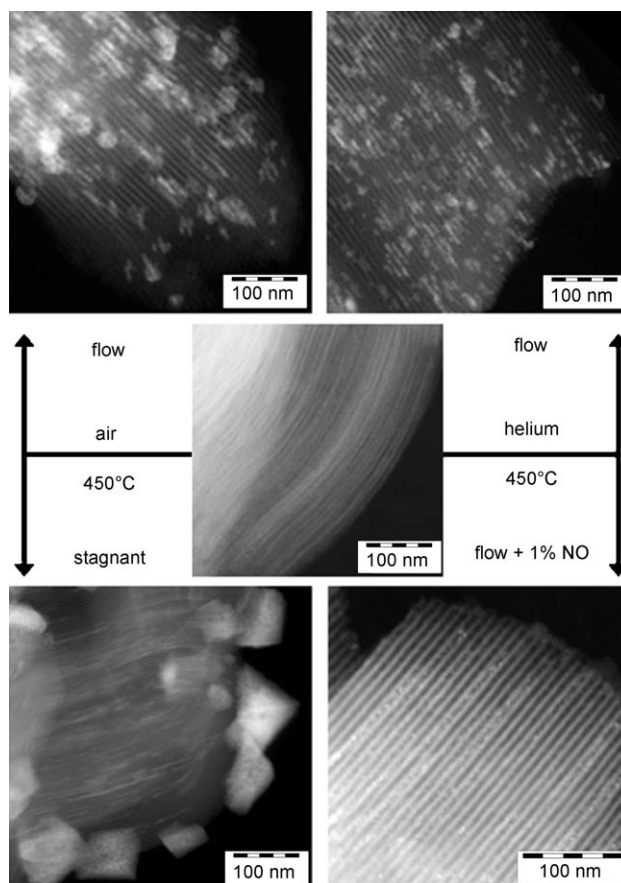


**Figure 1.** HAADF-STEM images of Ni<sub>3</sub>(NO<sub>3</sub>)<sub>2</sub>(OH)<sub>4</sub>/SBA-15 obtained after drying at 120 °C (center) and of NiO/SBA-15 obtained after different thermal treatments at 450 °C, as indicated.

[\*] J. R. A. Sietsma, J. P. den Breejen, M. Versluijs-Helder, Dr. A. J. van Dillen, Dr. P. E. de Jongh, Prof. K. P. de Jong  
Inorganic Chemistry and Catalysis  
Utrecht University  
Sorbonnelaan 16, 3584 CA, Utrecht (The Netherlands)  
Fax: (+31) 30-253-7400  
E-mail: k.p.dejong@chem.uu.nl  
J. D. Meeldijk  
Electron Microscopy Utrecht (EMU)  
Utrecht University  
Padualaan 8, 3584 CH, Utrecht (The Netherlands)

the precursor phase was found only inside the mesopores of the silica. The  $N_2$  physisorption results (Table 1) support these findings, as a significant decrease in mesoporosity was found.

**Table 1:** Selected  $N_2$  physisorption results for SBA-15 samples.

Sample	$V_{\text{meso}} [\text{cm}^3 \text{ g}_{\text{SiO}_2}^{-1}]^{[a]}$
SBA-15	0.68
$\text{Ni}_3(\text{NO}_3)_2(\text{OH})_4/\text{SBA-15}$	0.42
$\text{NiO}/\text{SBA-15}$ (air flow)	0.56
$\text{NiO}/\text{SBA-15}$ (NO/He flow)	0.49

[a] Mesopore volume calculated by the NL-DFT method.

This phase was identified as  $\text{Ni}_3(\text{NO}_3)_2(\text{OH})_4$ , with an average crystal size of 9 nm, by powder X-ray diffraction (XRD). This crystal size is close to the pore diameter of SBA-15 (9 nm), thereby indicating confinement by the pore walls. Subsequent heat treatment was carried out at 450 °C under atmospheres of different gases. Thermogravimetric analysis demonstrated that the decomposition of  $\text{Ni}_3(\text{NO}_3)_2(\text{OH})_4$  into NiO was complete in all cases.

Severe sintering and redistribution upon thermal decomposition in air (Figure 1, left) resulted in the formation of large NiO particles on the exterior surface of the support particles as well as rodlike NiO inside the mesopores.<sup>[11]</sup> Decomposition in a flow (top left) instead of stagnant air (bottom left) led to a decrease in the particle size range from 20–100 nm to 10–35 nm. These results are in line with the observations of Poels et al. and van de Loosdrecht et al., who have shown that removal of  $\text{NO}_x$  and  $\text{H}_2\text{O}$  decomposition products favors the formation of smaller particles.<sup>[6]</sup> Average crystal sizes of 25 and 10 nm were determined for the stagnant and flow samples, respectively, from the XRD patterns shown in Figure 2.

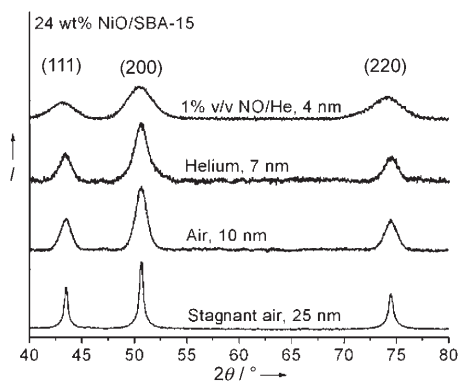


**Figure 2.** XRD patterns of 24 wt% NiO/SBA-15 obtained after thermal treatment at 450 °C under different atmospheres.

An STEM image obtained after thermal treatment under a flow of pure helium is also shown in Figure 1 (top right). The number and size of NiO particles (11–26 nm) on the exterior surface of the SBA-15 particles is significantly lower: the majority of particles are retained in the pores with a rodlike symmetry, although smaller particles are also present. The XRD peak shapes indicate a bimodal crystal-size distribution,

with an average crystal size of 7 nm. Thus, decomposition under an  $\text{O}_2$ -free flow significantly reduces aggregation, although it does not prevent it.

Finally, Figure 1 (bottom right) also shows the electron micrograph of a sample prepared by heating under a stream of helium containing NO (1% v/v). To the best of our knowledge, the use of NO to influence the thermal decomposition of nitrates has not been reported previously. Addition of NO to the helium feed resulted in the exclusive formation of small particles with a diameter of  $(4 \pm 1)$  nm; no rodlike particles were observed. XRD analysis (Figure 2) confirmed that NiO crystals with an average diameter of 4 nm had formed.

All samples were also analyzed by  $N_2$  physisorption, as the plugging of mesopores causes a typical desorption feature in the isotherm at  $P/P_0 \approx 0.48$ .<sup>[12]</sup> This feature was found for all samples except the NO/He treated ones, thus indicating that the NiO particles are smaller than 5 nm. Moreover, the mesopore volumes (Table 1) qualitatively support the STEM findings, as a lower porosity was found for the NO/He-treated samples than for the air-treated ones due to the more extensive retention of the NiO guest phase inside the mesopores. Hence, small and uniform NiO particles can be obtained in an NO/He flow.

We used in situ XRD to monitor the effect of the NO atmosphere on the rate of  $\text{Ni}_3(\text{NO}_3)_2(\text{OH})_4$  decomposition and NiO formation. The normalized peak areas of the  $\text{Ni}_3(\text{NO}_3)_2(\text{OH})_4$  (001) and NiO (200) diffraction lines obtained during isothermal decomposition at 248 °C in either an air or an NO/He (1% v/v) flow are shown in Figure 3. Decomposition proceeded relatively fast in the air flow, after an incubation time of about 25 minutes, and around 90% of the  $\text{Ni}_3(\text{NO}_3)_2(\text{OH})_4$  had decomposed within five minutes. Decomposition in an NO/He flow occurred at a rather constant rate and took almost 40 minutes. Thus, the NO/He flow prevents the delayed rapid decomposition observed in air.

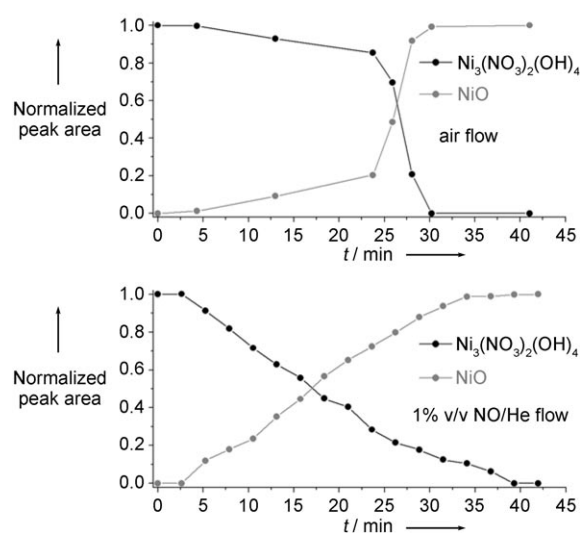


**Figure 3.** XRD results obtained in situ during the decomposition of  $\text{Ni}_3(\text{NO}_3)_2(\text{OH})_4$  into NiO at a constant temperature of 248 °C in either an air or an NO/He (1% v/v) flow.

Evolved-gas analysis by mass spectrometry showed predominantly the expected decomposition products given in Equation (2), except that no  $\text{O}_2$  was detected during decomposition in NO/He. This suggests that oxygen scavenging by NO is important and it is in line with the decrease in sintering when replacing air with helium.

Additional experiments under an NO/He or air atmosphere with conventional silica gel or carbon nanofibers as the support and cobalt nitrate as the precursor demonstrated the general applicability of our method, as similar results were obtained. The significance for catalysis was investigated by testing the Fischer–Tropsch activity of 18 wt % Co/SiO<sub>2</sub> catalysts prepared by reduction of Co<sub>3</sub>O<sub>4</sub> nanoparticles on silica gel. These particles were formed by cobalt nitrate decomposition either in an air (8–60-nm Co<sub>3</sub>O<sub>4</sub> particles) or in an NO/He (1% v/v) flow (4–5-nm Co<sub>3</sub>O<sub>4</sub> particles). The catalytic experiments were performed at 1 bar and 220 °C using synthesis gas (a mixture of H<sub>2</sub> and CO). Preparation of the catalyst by our new method led to an increase in activity by more than a factor of two, as the cobalt time yield increased from 2.4 to  $5.4 \times 10^{-5} \text{ mol}_{\text{CO}} \text{ g}_{\text{Co}}^{-1} \text{ s}^{-1}$ .

In conclusion, we have found a versatile method that allows the preparation of supported NiO and Co<sub>3</sub>O<sub>4</sub> particles with a diameter of 4–5 nm at relatively high loadings. This NO-moderated thermal decomposition of supported metal nitrates should therefore be a promising technique for the preparation of a wide range of metal (oxide) nanoparticles.

## Experimental Section

SBA-15 (pore volume of 1 mL g<sup>-1</sup>) was prepared according to the procedure reported by Stucky et al.<sup>[13]</sup> Davicat 1404 silica gel (SiO<sub>2</sub>; pore volume of 1.25 mL g<sup>-1</sup>) was obtained from Grace Davison. SBA-15 (0.25 g) or SiO<sub>2</sub> (1.00 g) was impregnated to incipient wetness with aqueous nickel (4.2 M) or cobalt nitrate (3 M) solution. The impregnates were dried for 12 h at 70 (Co) or 120 °C (Ni). The dried impregnate (40 mg for SBA-15 or 100 mg for SiO<sub>2</sub>) was then heated for 4 h at 450 °C, at a heating rate of 1 K min<sup>-1</sup>, in air, pure helium, or NO/He (1% v/v) at a flow rate of 90 mL min<sup>-1</sup>. Thermal decomposition in stagnant air was performed in a muffle oven in an oven dish with a lid on top.

STEM analysis was carried out with a Tecnai 20FEG microscope equipped with an HAADF detector (camera length: 120 mm). XRD measurements were performed with a Bruker-AXS D8 diffractometer equipped with a Co<sub>Kα1,2</sub> source. The experiments in situ were carried out with an Anton–Paar reaction chamber and gas flows of 90 mL min<sup>-1</sup>. Crystallite sizes were determined from the Scherrer equation with  $k = 1$ . N<sub>2</sub> physisorption isotherms were obtained at –196 °C with a Micromeritics Tristar 3000 apparatus. The samples were dried for 12 h at 120 °C prior to analysis. The mesopore volumes were calculated by the nonlocal density functional theory (NL-DFT) method of Jaroniec et al.,<sup>[14]</sup> which is included in the Micromeritics Datamaster software.

Fischer–Tropsch synthesis was performed at 1 bar and 220 °C in a plug-flow reactor (H<sub>2</sub>/CO = 2/1). The sample (20 mg) was diluted with 200 mg of SiC (0.2 mm) to achieve isothermal plug-flow conditions and reduced in situ in H<sub>2</sub>/He (33% v/v; 60 mL min<sup>-1</sup>) for 2 h at 550 °C

(ramp: 5 K min<sup>-1</sup>). Gas chromatography was used to determine the selectivity for C<sub>1</sub> and C<sub>5+</sub> hydrocarbons (wt %). The activities and selectivities were determined after 16 h of reaction. For this, the conversion of CO was adjusted to 2% by tuning the flows.

Received: February 9, 2007

Published online: May 3, 2007

**Keywords:** cobalt · nanostructures · nickel · nitric oxide · supported catalysts

- [1] a) P. Poizat, S. Laruelle, S. Grugeon, L. Dupont, J.-M. Tarascon, *Nature* **2000**, 407, 496–499; b) B. O'Regan, M. Grätzel, *Nature* **1991**, 353, 737–740; c) J. Kim, J. E. Lee, J. Lee, Y. Jang, S.-W. Kim, K. An, J. H. Yu, T. Hyeon, *Angew. Chem.* **2006**, 118, 4907–4911; *Angew. Chem. Int. Ed.* **2006**, 45, 4789–4793.
- [2] a) A. T. Bell, *Science* **2003**, 299, 1688–1691; b) R. Schlögl, S. B. Abd Hamid, *Angew. Chem.* **2004**, 116, 1656–1667; *Angew. Chem. Int. Ed.* **2004**, 43, 1628–1637; c) J. Y. Ying, *Chem. Eng. Sci.* **2006**, 61, 1540–1548.
- [3] N. K. Mal, N. Fuijwara, Y. Tanaka, *Nature* **2003**, 421, 350–353.
- [4] a) K. P. de Jong, *Curr. Opin. Solid State Mater. Sci.* **1999**, 4, 55–62; b) K. Bourikas, C. Kordulis, A. Lycourghiotis, *Catal. Rev. Sci. Eng.* **2006**, 48, 363–444; c) F. Négrier, E. Marceau, M. Che, J.-M. Giraudon, L. Gengembre, A. Löfberg, *J. Phys. Chem. B* **2005**, 109, 2836–2845; d) M. K. van der Lee, A. J. van Dillen, J. H. Bitter, K. P. de Jong, *J. Am. Chem. Soc.* **2005**, 127, 13573–13582; e) P. Burattin, M. Che, C. Louis, *J. Phys. Chem. B* **1999**, 103, 6171–6178.
- [5] A. J. van Dillen, R. J. A. M. Terörde, D. J. Lensveld, J. W. Geus, K. P. de Jong, *J. Catal.* **2003**, 216, 257–264.
- [6] a) E. K. Poels, J. G. Dekker, W. A. van Leeuwen, *Stud. Surf. Sci. Catal.* **1991**, 63, 205–214; b) J. van de Loosdrecht, S. Barradas, E. A. Caricato, N. G. Ngwenya, P. S. Nkwanyana, M. A. S. Rawat, B. H. Sigwebela, P. J. van Berge, J. L. Visagie, *Top. Catal.* **2003**, 26, 121–127.
- [7] P. A. Chernavskii, A. Y. Khodakov, G. V. Pankina, J.-S. Girardon, E. Quinet, *Appl. Catal. A* **2006**, 306, 108–119.
- [8] a) E. Iglesia, *Appl. Catal. A* **1997**, 161, 59–78; b) G. L. Bezemer, J. H. Bitter, H. P. C. E. Kuipers, H. Oosterbeek, J. E. H. H. Xu, F. Kapteijn, A. J. van Dillen, K. P. de Jong, *J. Am. Chem. Soc.* **2006**, 128, 3956–3964.
- [9] J. R. A. Sietsma, A. J. van Dillen, P. E. de Jongh, K. P. de Jong, *Stud. Surf. Sci. Catal.* **2006**, 95–102.
- [10] J. M. Thomas, P. A. Midgley, T. J. V. Yates, J. S. Barnard, R. Raja, I. Arslan, M. Weyland, *Angew. Chem.* **2004**, 116, 6913–6915; *Angew. Chem. Int. Ed.* **2004**, 43, 6745–6747.
- [11] a) E. L. Salabas, A. Rumpelcker, F. Kleitz, F. Radu, F. Schüth, *Nano Lett.* **2006**, 6, 2977–2981; b) L. Vradman, M. V. Landau, D. Kantorovich, Y. Koltypin, A. Gedanken, *Microporous Mesoporous Mater.* **2005**, 79, 307–318; c) V. Escax, M. Impérator-Clerc, D. Bazin, A. Davidson, *C. R. Chim.* **2005**, 8, 663–677.
- [12] a) P. I. Ravikovitch, A. V. Neimark, *Langmuir* **2002**, 18, 9830–9837; b) A. H. Janssen, C.-M. Yang, Y. Wang, F. Schüth, A. J. Koster, K. P. de Jong, *J. Phys. Chem. B* **2003**, 107, 10552–10556.
- [13] D. Zhao, J. Feng, Q. Huo, N. Melosh, G. H. Fredrickson, B. F. Chmelka, G. D. Stucky, *Science* **1998**, 279, 548–552.
- [14] M. Jaroniec, M. Kruk, J. P. Olivier, S. Koch, *Proceedings of COPS-V*, Heidelberg, Germany **1999**.